

Understanding the Sensing Mechanism of Rh₂O₃ loaded In₂O₃[†]

Inci Boehme *, Sina Herrmann, Anna Staerz, Helena Brinkmann, Udo Weimar and Nicolae Barsan

Institute of Physical and Theoretical Chemistry, Eberhard Karls University Tübingen, 72076 Tübingen, Germany; sina.herrmann@ipc.uni-tuebingen.de (S.H.); anna.staerz@student.uni-tuebingen.de (A.S.); helena.brinkmann@student.uni-tuebingen.de (H.B.); upw@ipc.uni-tuebingen.de (U.W.); nb@ipc.uni-tuebingen.de (N.B.)

* Correspondence: inci.boehme@ipc.uni-tuebingen.de; Tel.: +49-7071-2978766

† Presented at the Eurosensors 2018 Conference, Graz, Austria, 9–12 September 2018.

Published: 6 December 2018

Abstract: The effect of Rh loading on CO sensing was studied for the case of In₂O₃. This was done by performing measurements with sensors based on loaded and unloaded materials that were performed at an operation temperature of 300 °C in the presence of low background oxygen concentration according to an experimental procedure that was demonstrated to help clarify the reception/transduction functions of loaded Semiconducting Metal Oxides (SMOX). The experimental investigation methods were DC resistance and Diffuse Reflectance Infrared Fourier Transform Spectroscopy (DRIFTS). The results indicate that in the case of Rh₂O₃ loaded In₂O₃ the reaction primary takes place on the Rh₂O₃ cluster and the electrical properties of the In₂O₃ are controlled by the pinning of the SMOX Fermi-level to the one of the Rh₂O₃ cluster.

Keywords: In₂O₃; Rh₂O₃ loading; SMOX; gas sensors; DRIFTS; operando; surface chemistry

1. Introduction

Gas sensors based on noble metal loaded SMOX, such as Au, Pt, Pd or Rh, are utilized to solve many applications. The way in which the noble metal additives are influencing the sensitivity, selectivity as well as the stability of the SMOX gas sensors is a hot topic of research and there are many concepts discussed in the research community. On the opposite of the case of loaded SnO₂ and, lately, WO₃ very little is known about loaded In₂O₃ even if its sensing performance is quite interesting.

In order to gain fundamental insights on this topic, 0.5 and 1 at% Rh₂O₃-loaded In₂O₃, were chosen as model samples—the investigating approach is inspired by the work described in [1,2], because it was demonstrated that it helped the prevalence of a Fermi-level control mechanism that explained the gas sensing performance. Besides the loaded samples, an unloaded one was used as a reference; all sensors were operated at 300 °C. DC electrical resistance measurements and operando-DRIFTS investigations were performed during exposure to different concentrations of CO in a background of 50 ppm oxygen in N₂.

2. Materials and Methods

Unloaded sample. To have a reference and the same conditions as the loaded materials, the unloaded In₂O₃ sample, purchases from Sigma Aldrich, was prepared like the loaded material as follows: the powder was suspended in deionized water at a pH value of 1.0, stirred at 80 °C for two hours and dried at 70 °C. The powder is labeled pure-In₂O₃.

Rh_2O_3 -loaded samples. The 0.5 at% and 1.0 at% Rh_2O_3 loaded In_2O_3 were prepared as described in [3]: 1.5 g of In_2O_3 and 0.0055 g/0.0113 g of $\text{RhCl}_3 \cdot x\text{H}_2\text{O}$ from Sigma Aldrich were stirred in deionized water at a pH value of 1 at 80 °C for two hours and dried at 70 °C. The powders are labeled 0.5Rh- In_2O_3 and 1.0Rh- In_2O_3 for 0.5 at% Rh_2O_3 loaded In_2O_3 and 1.0 at% Rh_2O_3 loaded In_2O_3 , respectively. The three powders were deposited onto alumina substrates described elsewhere [4]. The DRIFTS measurements were performed at Bruker Vertex 80v at 300 °C under CO (25, 50, 10, 200 and 400 ppm) in nitrogen with 50 ppm oxygen in the background. DC resistance measurements were performed simultaneously. The displayed absorbance spectra were obtained by referring the single channel spectra under exposure to the target gases to the spectra gained under carrier gas:

$$\text{absorbance} = -\log(\text{sample spectrum}/\text{reference spectrum})$$

3. Results and Discussion

Figure 1 shows the DC resistance measurements and DRIFTS absorbance spectra of the three sensors during the exposure to CO in nitrogen with 50 ppm oxygen. At the first glance, the DC resistance measurements in Figure (1a) reveal an influence of the loading on the baseline resistance: most probably, the p-n-heterojunction between the Rh_2O_3 cluster and In_2O_3 support material leads to a diffusion of the electrons of In_2O_3 to the noble metal oxide cluster to balance the Fermi-levels of both materials. This is followed by a depletion layer and consequently a higher baseline resistance.

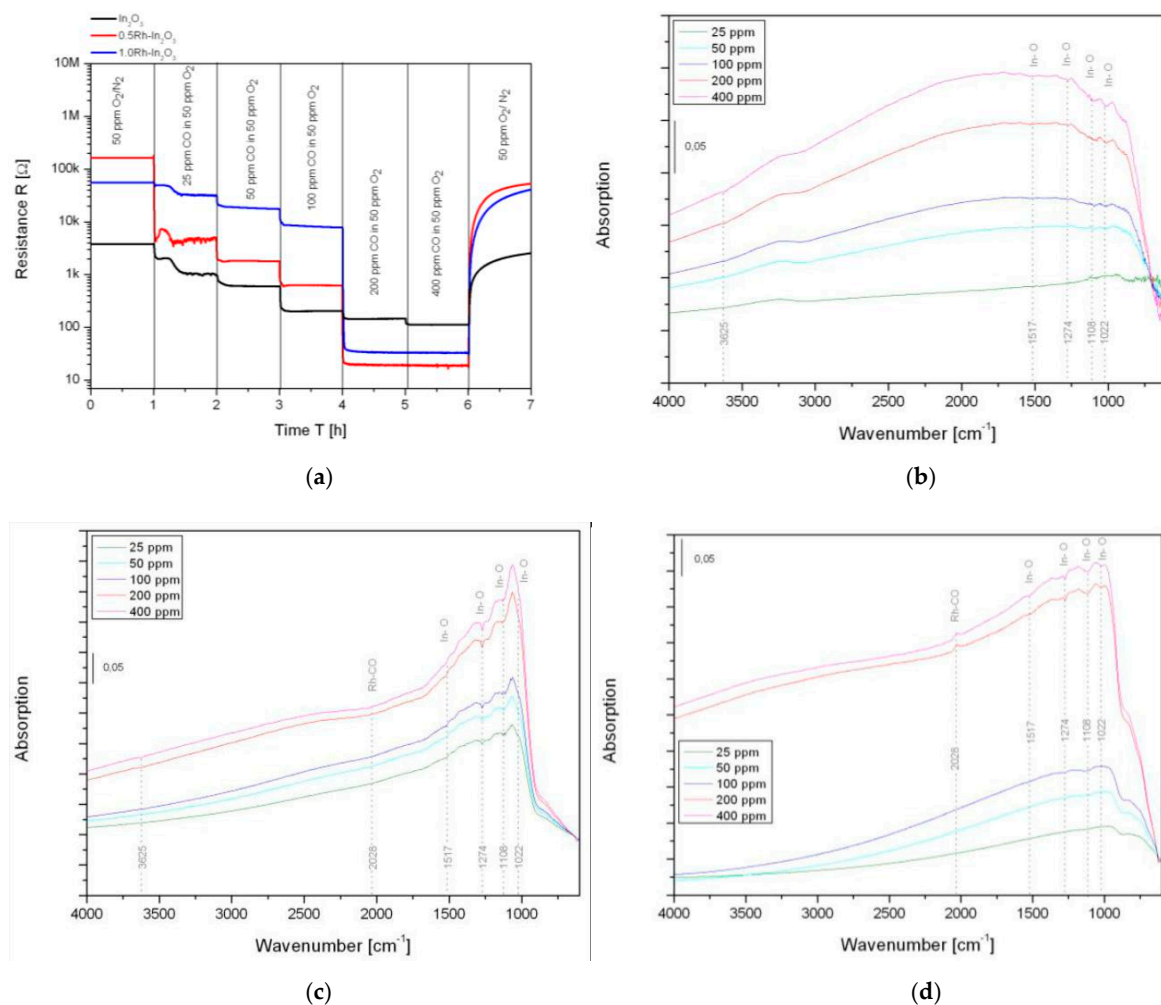
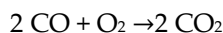


Figure 1. (a) DC resistance measurement of pure- In_2O_3 , 0.5Rh- In_2O_3 and 1.0Rh- In_2O_3 under 25, 50, 100, 200 and 400 ppm CO in nitrogen with 50 ppm oxygen in the background. Absorbance spectra of (b) pure- In_2O_3 , (c) 0.5Rh- In_2O_3 and (d) 1.0Rh- In_2O_3 under 25, 50, 100, 200 and 400 ppm CO in nitrogen with 50 ppm oxygen in the background, reference spectra: nitrogen with 50 ppm oxygen.

The chosen CO concentrations correspond to below (25 and 50 ppm), nearly (100 ppm) and above (200 and 400 ppm) the stoichiometric conditions for the oxidation of CO to CO₂:



In these conditions, all sensors show a reduction of the resistance with increasing CO concentration. While for pure-In₂O₃ the decrease of the DC resistance proceeds gradually, for 0.5Rh-In₂O₃, however, a slight drop is observable when the CO concentration exceeds the stoichiometric conditions. For 1.0Rh-In₂O₃, the drop in the resistance is more pronounced.

The simultaneously acquired DRIFT spectra reveal a change in the sensing mechanisms: in the case of pure-In₂O₃ in Figure (1b) all CO concentration exposures determine the decrease of the In-O bands centered at 1517, 1274, 1108 and 1022 cm⁻¹ [5]. This indicates the reduction of the surface of this material. For 0.5Rh-In₂O₃, which is shown in Figure (1c), the decrease of the In-O bands appear for all CO concentrations as well, but in this case, as soon as the conditions in which the slight drop in the resistance is observed, an additional band centered at 2028 cm⁻¹ appears. This can be assigned to a rhodium carbonyl Rh-CO group [6]. A similar observation can be made for 1.0Rh-In₂O₃ in Figure (1d), but this time, the decrease of the In-O bands appear just in the same conditions in which the large drop in the resistance was observed, thus beyond the stoichiometric conditions. At this point, also here the occurrence of Rh-CO band can be observed. These observations indicate that the reaction primarily takes place on the Rh₂O₃ cluster—when the stoichiometric conditions are reached and exceeded, the Rh₂O₃ clusters are fully reduced to metallic Rh (indicated by the Rh-CO band) since they cannot be reoxidized and the reaction moves to the surface of In₂O₃ (indicated by the decreasing In-O bands).

In the literature, two reaction mechanisms are considered: the spill over mechanism and the Fermi-level pinning. In the spill over mechanism, the molecule is adsorbed on the noble metal cluster. This leads to a weakening of the molecular bond and the spillover of the so prepared adsorbate onto the support material where the reaction takes place [7]. In the Fermi-level pinning, the gas detection reaction takes place on the surface of the noble metal cluster, which interacts with the SMOX with a different work function. The contact pins the Fermi-levels of the two materials. If the electrical property of the noble metal cluster is changed, the depletion caused by the contact is changed as well. This will cause a change in the resistance of the sensing layer [8]. The findings, made in this work, suggest that the Fermi-level pinning dominates the sensing mechanism: it could be indirectly shown that the reaction takes place on the Rh₂O₃ cluster. As soon as the cluster is fully reduced to metallic Rh, the reaction is released on In₂O₃, indicated by the decreasing In-O bands in overstoichiometric conditions where the noble metal cluster cannot be reoxidized.

4. Conclusions

It is shown that it is spectroscopically possible to understand the reaction mechanism of loaded In₂O₃ gas sensing material. The results are in line with the findings for Pt-loaded SnO₂ and Rh-loaded WO₃ and suggest that the Fermi-level control can also be assumed for the loading of In₂O₃ with Rh₂O₃.

Author Contributions: All authors contributed equally to this work.

Conflicts of Interest: The authors declare no conflict of interest.

References

1. Staerz, A.; Kim, T.-H.; Lee, J.-H.; Weimar, U.; Barsan, N. Nanolevel Control of Gas Sensing Characteristics via p–n Heterojunction between Rh₂O₃ Clusters and WO₃ Crystallites. *J. Phys. Chem. C* **2017**, *121*, 24701–24706. doi:10.1021/acs.jpcc.7b09316.
2. Degler, D.; Müller, S.A.; Doronkin, D.E.; Wang, D.; Grunwaldt, J.D.; Weimar, U.; Barsan, N. Platinum loaded tin dioxide: A model system for unravelling the interplay between heterogeneous catalysis and gas sensing. *J. Mater. Chem. A* **2018**, *6*, 2034–2046. doi:10.1039/c7ta08781k.

3. Choi, K.-I.; Hwang, S.-J.; Dai, Z.; Kang, Y.C.; Lee, J.-H. Rh-catalyzed WO₃ with anomalous humidity dependence of gas sensing characteristics. *RSC Adv.* **2014**, *4*, 53130–53136. doi:10.1039/C4RA06654E.
4. Wicker, S.; Guiltat, M.; Weimar, U.; Hémerlyck, A.; Barsan, N. Ambient Humidity Influence on CO Detection with SnO₂ Gas Sensing Materials. A Combined DRIFTS/DFT Investigation. *J. Phys. Chem. C* **2017**, *121*, 25064–25073. doi:10.1021/acs.jpcc.7b06253.
5. Can, I.; Weimar, U.; Barsan, N. Operando Investigations of Differently Prepared In₂O₃-Gas Sensors. *Proceedings* **2017**, *1*, 432. doi:10.3390/proceedings1040432.
6. Hecker, W.C.; Rasband, P.B. Catalyst Characterization Using Quantitative FTIR: CO on Supported Rh. *J. Catal.* **1993**, *139*, 551–560. doi:10.1006/jcat.1993.1048.
7. Matsushima, S.; Teraoka, Y.; Miura, N.; Yamazoe, N. Electronic interaction between metal additives and tin dioxide in tin dioxide-based gas sensors. *Jpn. J. Appl. Phys.* **1988**, *27*, 1798–1802. doi:10.1143/JJAP.27.1798.
8. Yamazoe, N.; Kurokawa, Y.; Seiyama, T. Effects of Additives on Semiconductor Gas Sensors. *Sens Actuator* **1983**, *4*, 283–289, doi:10.1016/0250-6874(83)85034-3.



© 2018 by the authors. Licensee MDPI, Basel, Switzerland. This article is an open access article distributed under the terms and conditions of the Creative Commons Attribution (CC BY) license (<http://creativecommons.org/licenses/by/4.0/>).